Available online at www.sciencedirect.com
SCIENCE DIRECT®
Physica B 340–342 (2003) 39–47
PHYSICA B
www.elsevier.com/locate/physb

Effects of defects and doping on wide band gap ferromagnetic semiconductors

S.J. Pearton[a,*], C.R. Abernathy[a], G.T. Thaler[a], R. Frazier[a], F. Ren[b], A.F. Hebard[c], Y.D. Park[d], D.P. Norton[a], W. Tang[e], M. Stavola[e], J.M. Zavada[f], R.G. Wilson[g]

[a] *Department of Materials Science and Engineering, University of Florida, P.O. Box 116400, Gainesville, FL 32611 USA*
[b] *Department of Chemical Engineering, University of Florida, Gainesville, FL 32611 USA*
[c] *Department of Physics, University of Florida, Gainesville, FL 32611 USA*
[d] *Center for Strongly Correlated Materials Research, Seoul 151-747, South Korea*
[e] *Physics Department, Lehigh University, Bethlehem, PA 18015 USA*
[f] *US Army Research Office, Research Triangle Park, NC 27709, USA*
[g] *Consultant, Stevenson Ranch, CA 91381 USA*

Abstract

Both ion implantation and epitaxial crystal growth provide convenient methods of introducing transition metals such as Mn,Cr,Fe,Ni and Co into GaN, GaP, SiC and ZnO for creating dilute magnetic semiconductors exhibiting room temperature ferromagnetism. In this paper we review progress in wide band gap ferromagnetic semiconductors and the role of defects and doping on the resulting magnetic properties.
© 2003 Elsevier B.V. All rights reserved.

Keywords: Defects; Doping; Ferromagnetism; Wide band gap; Semiconductors

1. Introduction

The use of electron spin, in addition its more commonly used charge, holds great promise for a new class of semiconductor memory and signal processing devices with new functionality [1–7]. For a long period electron spin in metals has been exploited in information storage and in particular the giant magneto-resistance (GMR) effect, where the resistance of a thin-film ferromagnetic/non-magnetic layer sandwich is strongly magnetic field dependent [8] is used in most computer hard drives. In recent years, attention has also focused on spin-dependent phenomena in semiconductors. A potential device embodiment is the spin field effect transistor (FET) in which the drain and source of a conventional FET are ferromagnetic [9]. If the two ferromagnets are aligned, a spin-polarized current will behave like a normal FET current. If the ferromagnets are anti-aligned, the transistor will be shut off. This could be done dynamically, allowing for microprocessors that reconfigure their hardware in real time.

A major hindrance for the practical implementation of the above concepts is that they require

*Corresponding author. Tel.: 3528461086; fax: 3528461182.
E-mail address: spear@mse.ufl.edu (S.J. Pearton).

0921-4526/$ - see front matter © 2003 Elsevier B.V. All rights reserved.
doi:10.1016/j.physb.2003.09.003

efficient spin-polarized carrier injection and transport. Conventional ferromagnetic metals are often incompatible with existing semiconductor technology. Moreover, the spin injection efficiency is often very low due to resistivity differences and to the formation of Schottky barriers [10,11]. A key materials aspect to overcoming this problem is the use of dilute magnetic semiconductors (DMSs). These materials are alloys where a stoichiometric fraction of the constituent atoms has been replaced by transition metal atoms. Such alloys are semiconducting, but can possess well-defined magnetic properties (e.g., paramagnetic, antiferromagnetic, ferromagnetic) that conventional semiconductors do not have [1,6,7]. Thus, they can potentially serve as a means to inject spin to and control spin properties in adjacent non-magnetic semiconducting layers.

Most of the initial work in this area has been performed on II–VI semiconductors of the form $A_{1-x}{}^{II}Mn_xB^{VI}$, in which a fraction of the group II sub-lattice is randomly replaced by Mn atoms. The presence of magnetic ions in such systems affects the free carrier behavior through the sp–d exchange interaction between the localized magnetic moments and the spins of the itinerant carriers. These interactions have resulted in the discovery of numerous magneto-electrical and magneto-optical phenomena, including GMR, large Faraday rotation and magnetic polaron formation [11].

The use of molecular beam epitaxy (MBE) to grow $Mn_xGa_{1-x}As$ has allowed incorporation of Mn fractions up to 0.1, well in excess of the miscibility limit of Mn in this material [12]. The resulting alloy was found to be ferromagnetic with a Curie temperature of $\sim$110 K. Numerous phenomena related to DMS/semiconductor heterostructures have been reported including spin-injection from MnGaAs to GaAs and electrically controlled magnetism in MnInAs [12–14].

2. Ferromagnetism in semiconductors

Magnetism in semiconductor materials has been studied for many years, and includes spin glass and antiferromagnetic behavior in Mn-doped II–VI compounds, as well as ferromagnetism in europium chalcogenides and Cr-based spinels [15,16]. Strong ferromagnetic interaction between localized spins has been observed in Mn-doped II–VI compounds with high carrier densities. In $Pb_{1-x-y}Sn_yMn_xTe$ ($y > 0.6$) possessing a hole concentration of the order of 10^{20}–10^{21} cm^{-3}, ferromagnetism has been achieved [17]. In addition, it has been shown that free holes in low-dimensional structures of II–VI DMSs can induce ferromagnetic order [18]. For many semiconductor materials, the bulk solid solubility for magnetic and/or electronic dopants is not conducive with the coexistence of carriers and spins in high densities. However, the low solubility for transition metals in semiconductors can often be overcome via low temperature epitaxial growth. Behavior indicative of ferromagnetism at temperatures above 300 K has recently been reported for GaN and chalcopyrite semiconductors doped with transition metals, illustrating the potential of achieving room temperature spintronics technologies [19,20].

Despite recent experimental success, a fundamental description of ferromagnetism in semiconductors remains incomplete. Recent theoretical treatments have yielded useful insight into fundamental mechanisms. Dietl et al. [21] have applied Zener's model for ferromagnetism, driven by exchange interaction between carriers and localized spins, to explain the ferromagnetic transition temperature in III–V and II–VI compound semiconductors. The theory assumes ferromagnetic correlations mediated by holes from shallow acceptors in a matrix of localized spins in a magnetically doped semiconductor. Specifically, Mn ions substituted on the group II or III site provide the local spin. In the case of III–V semiconductors, Mn also provides the acceptor dopant. High concentrations of holes are believed to mediate the ferromagnetic interactions among Mn ions. Direct exchange among Mn is antiferromagnetic as observed in fully compensated (Ga,Mn)As that is donor-doped. In the case of electron doped or heavily Mn doped materials, no ferromagnetism is detected. Theoretical results suggest that carrier-mediated ferromagnetism in n-type material is relegated to low temperatures, if it occurs at all, while it is predicted at higher

temperatures for p-type materials [22]. In p-type GaAs grown by low temperature MBE, Mn doping in the concentration range $0.04 \leqslant x \leqslant 0.06$ results in ferromagnetism in GaAs. The model described has been reasonably successful in explaining the relatively high transition temperature observed for (Ga,Mn)As.

Carrier-mediated ferromagnetism in semiconductors is dependent on the magnetic dopant concentration as well as on the carrier type and carrier density. As these systems can be envisioned as approaching a metal–insulator transition when carrier density is increased and ferromagnetism is observed, it is useful to consider the effect of localization on the onset of ferromagnetism. As carrier density is increased, the progression from localized states to itinerant electrons is gradual. On the metallic side of the transition, some electrons populate extended states while others reside at singly occupied impurity states. On crossing the metal–insulator boundary, the extended states become localized, although the localization radius gradually decreases from infinity. For interactions on a length scale smaller that the localization length, the electron wave function remains extended. In theory, holes in extended or weakly localized states could mediate the long-range interactions between localized spins. This suggests that for materials that are marginally semiconducting, such as in heavily doped semiconducting oxides, carrier-mediated ferromagnetic interactions may be possible. This theoretical treatment presents several interesting trends and predictions. For the materials considered in detail (semiconductors with zinc-blende structure), magnetic interactions are favored in hole-doped materials due to the interaction of Mn^{+2} ions with the valence band. This is consistent with previous calculations for the exchange interaction between Mn^{+2} ions in II–VI compounds [11,22] showing that the dominant contribution is from two-hole processes. This superexchange mechanism can be viewed as an indirect exchange interaction mediated by the anions, thus involving the valence band. Note that valence band properties are primarily determined by anions in II–VI compounds. The model by Dietl et al. predicts that the transition temperature will scale with a reduction in the atomic mass of the constituent elements due to an increase in p–d hybridization and a reduction in spin–orbit coupling. Most importantly, the theory predicts a T_c greater than 300 K for p-type GaN and ZnO, with T_c dependent on the concentration of magnetic ions and holes. Recent experimental evidence for ferromagnetism in GaN appears to substantiate the theoretical arguments [23–31].

3. Computational approaches

The initial theories were based on spin-polarized density functional theory, in which the N-electron problem is mapped into an effective one-electron problem. All non-classical electron interactions, exchange and correlation, are subsumed into an additive one-electron potential that is a functional of the charge density. The exchange potentials include the spin-up and spin-down contributions, which lump all non-classical electron interaction into an additive potential term that depends only on the spin-up and spin-down charge densities. A schematic of some possible mechanisms for carrier-induced ferromagnetism is shown in Fig. 1, which contrast the mean-field approach with the bound magnetic polaron approach. An additional class of theories suggests that microscopic metallic clusters are responsible for the observed magnetic properties. The initial predictions from mean-field theory suggested that wide band gap semiconductors would have the potential for room temperature ferromagnetism when doped with a few percent of transition metal ions such as Mn. A

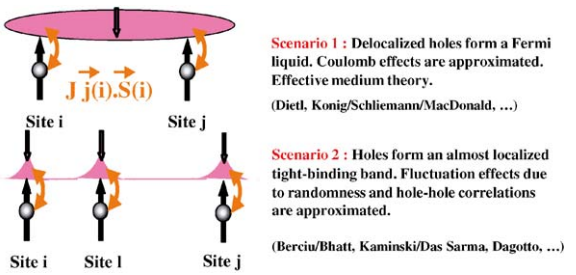

Fig. 1. Schematic of role of carriers (holes) in the various theories for carrier-induced ferromagnetism in dilute magnetic III–V semiconductors.

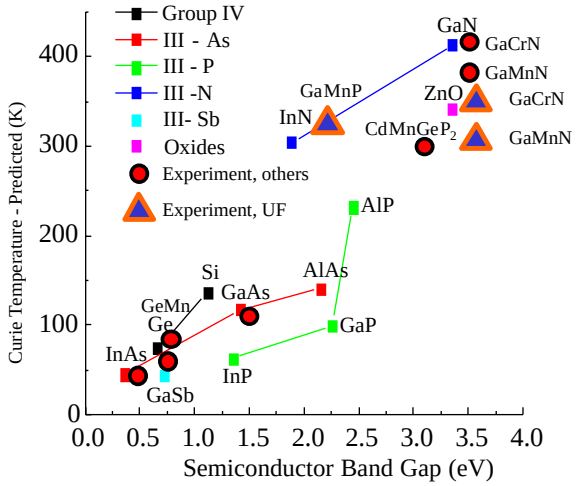

Fig. 2. Predicted Curie temperatures as a function of band gap (after Ref. [80]), along with some experimentally reported values in the literature.

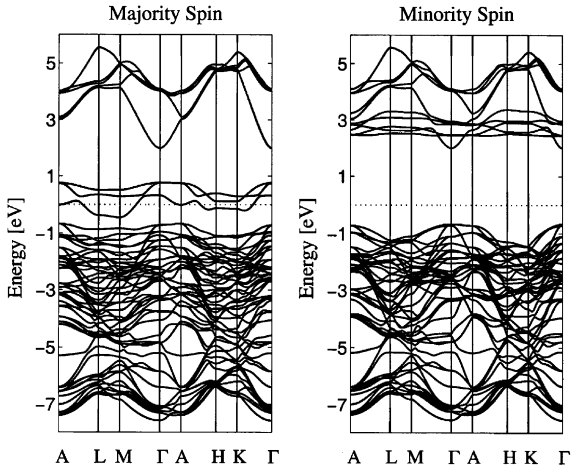

Fig. 3. Computed band structure diagrams of wurtzite $Mn_{0.063}Ga_{0.937}N$ along selected high symmetry directions in the Brillouin zone.

compilation of these predictions with some experimental data is shown in Fig. 2.

Numerous calculations of the properties of DMSs in their ordered ferromagnetic phase have been reported. An example is given in Fig. 3, which shows band structure diagrams for wurtzite $Mn_{0.063}Ga_{0.937}N$ [32,33]. The material is found to be half-metallic in that the majority spin possesses a Fermi surface whereas the minority spin does not. This is an ideal situation for use in spintronics, since in this case charge carriers injected from the vicinity of the Fermi level will have a well-defined spin. The nature of the spin-polarized feature is very different from that of GaMnAs with the same concentration of Mn. In that case, the spin polarized feature is narrow and corresponds to a spin-split valence band, whereas in $Mn_{0.063}Ga_{0.937}N$ it is wide and corresponds to a hybridized impurity band. The GaMnN is predicted to be half-metallic and an ideal spin injector. The ferromagnetic states are predicted to be stable over the spin-glass states and ferromagnetism is expected to be attainable even at low carrier concentrations. We have measured the Mn acceptor level as being at $E_V + 1.4$ eV, so that it is ineffective at contributing holes and to obtain p-type doping it will be necessary to co-dope with Mn.

4. Methods of transition metal incorporation

Both ion implantation and doping during epitaxial growth can be used successfully to incorporate the magnetic ions. Ion implantation is particularly useful for surveying the properties of many different transition metal dopants in semiconductors because of the ease of incorporation. Fig. 4 shows the status of the available elements in the Periodic Table that can be implanted into semiconductors. We have used Mn, Cr, V, Fe, Ni and Co to date, and the results can be a useful check on theories that suggest only some of these elements will stabilize in the ferromagnetic state in particular semiconductors.

5. GaMnN

Numerous groups have demonstrated room temperature ferromagnetism in n-type and p-type GaN doped with Mn by diffusion, ion implantation or during epitaxial growth [23–31], as summarized in Table 1. This table also shows a compilation of other semiconductors that have exhibited room temperature ferromagnetism. The advantages of using GaMnN include compatibility

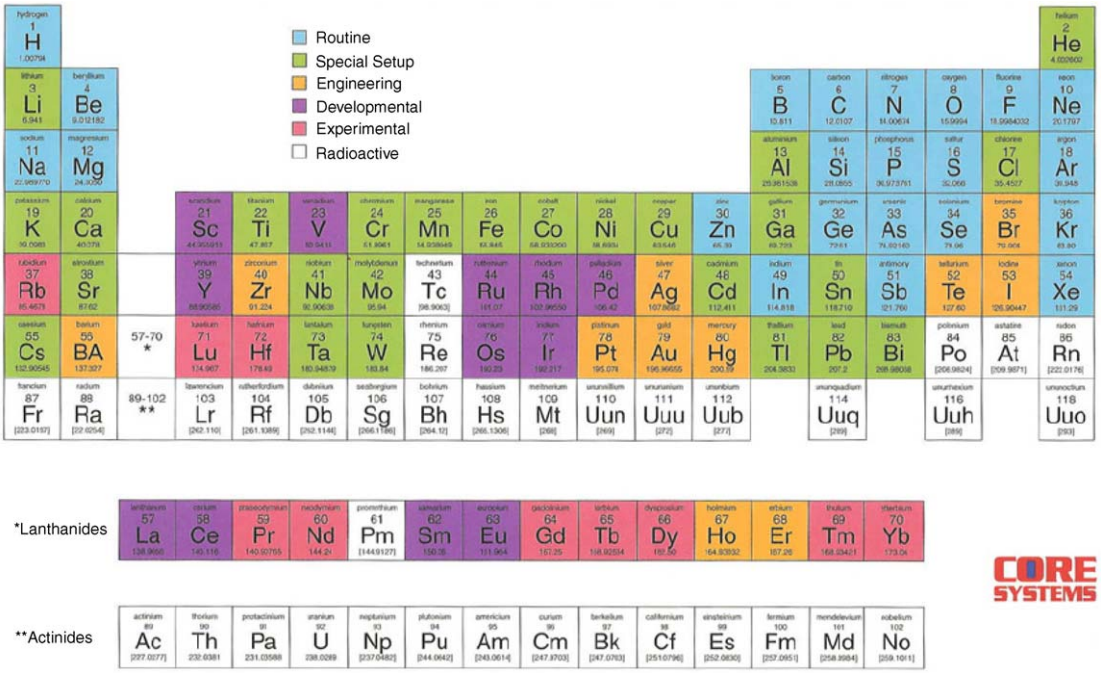

Fig. 4. Schematic showing availability of different elements for implantation.

Table 1
Compilation of semiconductors showing room temperature ferromagnetism

Material	Band gap of host (eV)	Comments	Ordering Temperature (K)	Ref.
$Cd_{1-x}Mn_xGeP_2$	1.72	Solid-phase reaction of evap. Mn	> 300	[36]
(Ga,Mn)N	3.4	Mn incorporated by diffusion	228–370	[23]
(Ga,Mn)N	3.4	Mn incorporated during MBE; n-type	> 300	[25]
(Ga,Mn)N	3.4	Mn incorporated during MBE	940[a]	[26]
(Ga,Cr)N	3.4	Cr incorporated during MBE or bulk growth	> 400	[37]
(ZnO):Co	3.1–3.6	Co incorporated during PLD; ~15% Co	> 300	[38]
(Al,Cr)N	6.2	Cr incorporated during MBE, sputtering or implantation	> 300	[39]
(Ga,Mn)P:C	2.2	Mn incorporated by implant or MBE; $p \sim 10^{20}$ cm^{-3}	> 330	[40,41]
$(Zn_{1-x}Mn_x)GeP_2$	1.83–2.8	Sealed ampule growth; insulating; 5.6% Mn	312	[42]
$(ZnMn)GeP_2$	<2.8	Mn incorporated by diffusion	350	[43]
$ZnSnAs_2$	0.65	bulk growth	329	[44]
$ZnSiGeN_2$	3.52	Mn-implanted epi	~300	[45]
SiC	3. 2	Mn or Fe implantation	~300 (by hysteresis)	[46]

[a] Extrapolated from measurements up to ~750 K.

with current III–N applications such as high temperature/high power electronics and blue/green/UV lasers and light-emitting diodes. Extended X-ray absorption fine structure (EXAFS) measurements finds that the Mn is primarily substitutional on the Ga site and that post-growth annealing can increase the concentration of Mn in clustered form [34]. In growth by MBE, we have found that as the growth temperature increases, the maximum concentration of Mn that be incorporated while retaining a single-phase decreases. For example, for growth at 900°C, second phases form for Mn concentrations above ~3 at%, while at 700°C, the solubility limit is ~9 at%. For lower concentrations, no clusters can be detected by high resolution TEM, SADP or XRD. Fig. 5 shows that for growth at 700°C, the lattice constant is a minimum at 3 at% Mn and the X-ray FWHM increases. At this concentration, the band gap is increased by about 20 meV and the magnetic moment per Mn is $\sim 1\mu_B$. As the Mn concentration is increased, the lattice constant increases, FWHM decreases, the band gap remains unchanged and the moment per Mn decreases, all of which suggests that the concentration of substitutional Mn saturates at 3 at% and the additional Mn is probably in interstitial form. The type of buffer employed also has a strong influence on the resulting magnetic properties. For growth directly on sapphire, there is little or no magnetization detected, for growth on thin MBE low temperature buffers the magnetization is modest, while the best results are found for growth of the GaMnN on thick (3 μm) MOCVD buffers on sapphire. The field-cooled and zero-field-cooled magnetization is shown for such a sample in Fig. 6. The film morphology is also much smoother under these conditions. The resisitivity of the GaMnN at a given Mn concentration increases with decreasing growth temperature, with all films being n-type or resistive.

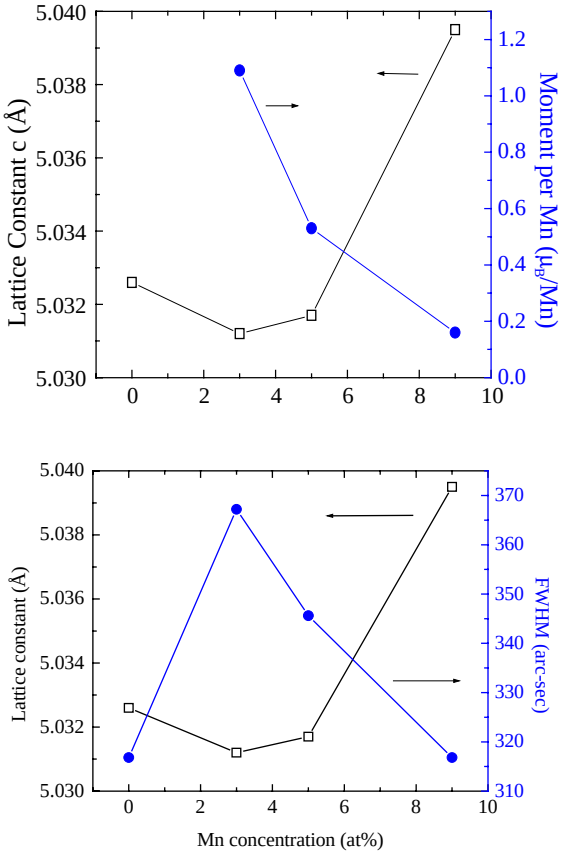

Fig. 5. Effect of Mn concentration on lattice constant, XRD FWHM and moment per Mn for GaMnN grown by MBE.

Co-doping with oxygen is also found to enhance the strength of the magnetization. Fig. 7 shows hysteresis loops at room temperature for films prepared with and without 8 at% O incorporated with 3 at% Mn. Without oxygen, the magnetic moment is about $0.06\mu_B$/Mn while this increases

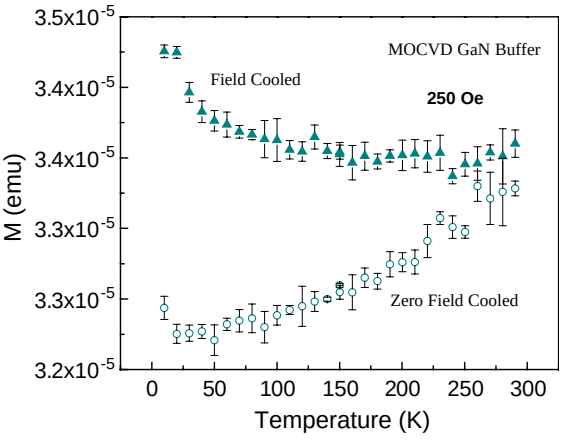

Fig. 6. Field-cooled and zero-field-cooled magnetization as a function of temperature for GaMnN with 3 at%. Mn grown by MBE on an MOCVD GaN buffer on sapphire.

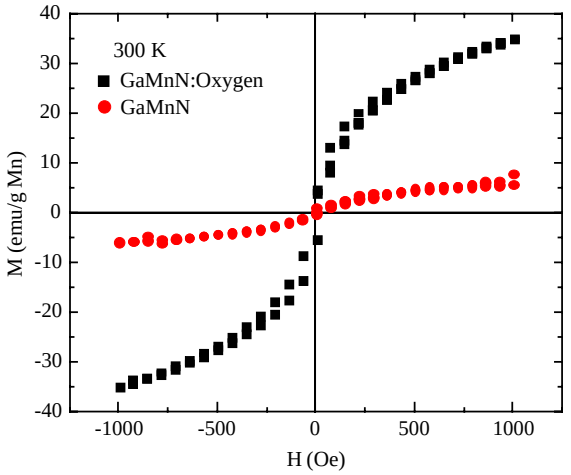

Fig. 7. Room temperature hysteresis loops from GaMnN grown either with or without co-doping with O.

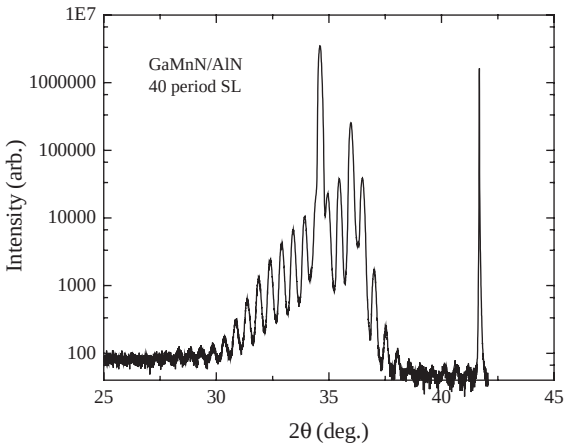

Fig. 8. XRD spectrum from 40 period GaMnN/AlN superlattice.

to $0.35\mu_B$ with the oxygen co-doping. This is consistent with theoretical predictions [35], but more characterization is needed to determine if the role of the oxygen is to enhance the Mn substitutionality.

It is of particular interest to develop thin DMS layers for device applications. Fig. 8 shows an XRD spectrum from a 40 period 10 nm AlN/10 nm GaMnN superlattice. The spectrum is indicative of good interfacial quality. The magnetic moment of the superlattice structure was approximately half that of a single layer GaMnN film of the same total thickness, demonstrating that ordering in 10 nm layers remains adequate for transport and device experiments. Detailed examination of the origin of the ferromagnetism in AlMnN films has shown that second phases of AlMn or Mn_4N are not responsible, through comparison with the magnetic properties of those materials synthesized by MBE. Of additional interest from the viewpoint of device fabrication is the fact that GaMnN is unstable against rapid thermal annealing at 800°C, so that alloying of ohmic contacts must be done at lower temperatures. There are still no convincing demonstrations of spin injection from GaMnN into GaN based devices.

6. Summary

Many groups have now demonstrated room temperature ferromagnetism in a variety of wide band gap semiconductors, of which GaMnN appears to have the best chance of utility in device applications. The crystal quality of the material is key to obtaining strong magnetization and lower growth temperature and higher V/III ration during MBE growth produce the highest concentrations of substitutional Mn. The use of O or Mg co-doping appears to be beneficial, while Si doping is ineffective in increasing magnetization. The best quality GaMnNn is still resistive and shows thermal stabilities of <800°C. Future work needs to focus on the achievement of p-type layers, the origin of the ferromagnetism, spin injection efficiencies and the utilization of this material in device structures.

Acknowledgements

The work at UF was partially supported by NSF-DMR 0101438, NSF-DMR 0101856, ARO-DAAD 190210420 while the work at SNU was partially supported by KOSEF and Samsung Electronics Endowment through CSCMR and by the Seoul National University Research Foundation. The work at Lehigh is partially supported by NSF DMR-0108914. The authors are very grateful

to their collaborators M.E. Overberg, Jihyun Kim, N.A. Theodoropoulou, R. Rairigh, J. Kelly, S.N.G. Chu, J.S. Lee and Z.G. Khim.

References

[1] S.A. Wolf, D.D. Awschalom, R.A. Buhrman, J.M. Daughton, S. von Molnar, M.L. Roukes, A.Y. Chtchelkanova, D.M. Treger, Science 294 (2001) 1488.
[2] D.D. Awschalom, D. Loss, N. Samarth (Eds.), Semiconductor Spintronics and Quantum Computation, Springer, Berlin, 2002.
[3] P. Ball, Nature 404 (2000) 918.
[4] D.D. Awschalom, J.M. Kikkawa, Phys. Today 52 (1999) 33;
D.D. Awschalom, M.E. Flatté, N. Samarth, Sci. Am. 286 (2002) 67.
[5] S. von Molnar, D. Read, J. Magn. Magn. Mater. 242–245 (2002) 13.
[6] S.J. Pearton, C.R. Abernathy, M.E. Overberg, G.T. Thaler, D.P. Norton, N. Theodorpoulou, A.F. Hebard, Y.D. Park, F. Ren, J. Kim, L.A. Boatner, J. Appl. Phys. 93 (2003) 1.
[7] S.J. Pearton, C.R. Abernathy, D.P. Norton, A.F. Hebard, Y.D. Park, L.A. Boatner, J.D. Budai, Mater. Sci. Eng. R 40 (2003) 137.
[8] M. Baibich, et al., Phys. Rev. Lett. 61 (1988) 2472;
J. Barnas, A. Fuss, R. Camley, P. Grunberg, W. Zinn, Phys. Rev. B 42 (1990) 8110.
[9] S. Datta, B. Das, Appl. Phys. Lett. 56 (1990) 665.
[10] G. Burkard, D. Loss, D.P. DiVincenzo, Phys. Rev. B 59 (1999) 2070.
[11] R.K. Willardson, A.C. Beer (Series Editors) J.K. Furdyna, J. Kossut (Volume Editors) Semiconductors and Semimetals, Vol. 25: Dilute Magnetic Semiconductors. Academic Press, Boston, 1988;
J.K. Furdyna, J. Appl. Phys. 64 (1988) R29;
M. Jain, Editor, Diluted Magnetic Semiconductors, World Scientific, Singapore, 1991.
[12] H. Ohno, Science 281 (1988) 951, and references therein.
[13] Y. Ohno, D.K. Young, B. Beschoten, F. Matsukura, H. Ohno, D.D. Awschalom, Nature 402 (1999) 790;
B. Beschoten, P.A. Crowell, I. Malajovich, D.D. Awschalom, F. Matsukura, A. Shen, H. Ohno, Phys. Rev. Lett. 83 (1999) 3073.
[14] H. Ohno, et al., Nature 408 (2000) 944.
[15] S. Gopalan, M.G. Cottam, Phys. Rev. B 42 (1990) 10311.
[16] C. Haas, Crit. Rev. Solid State Sci. 1 (1970) 47.
[17] T. Suski, J. Igalson, T. Story, J. Magn. Magn. Mater. 66 (1987) 325.
[18] A. Haury, A. Wasiela, A. Arnoult, J. Cibert, S. Tatarenko, T. Dietl, Y. Merle d'Aubigne, Phys. Rev. Lett. 79 (1997) 511;
P. Kossacki, D. Ferrand, A. Arnoult, J. Cibert, S. Tatarenko, A. Wasiela, Y. Merle d'Aubigne, J.-L. Staihli, J.-D. Ganiere, W. Bardyszewski, K. Swiatek, M. Sawicki, J. Wrobel, T. Dietl, Physica E 6 (2000) 709.
[19] K. Sato, G.A. Medvedkin, T. Nishi, Y. Hasegawa, R. Misawa, K. Hirose, T. Ishibashi, J. Appl. Phys. 89 (2001) 7027.
[20] M.E. Overberg, B.P. Gila, G.T. Thaler, C.R. Abernathy, S.J. Pearton, N.A. Theodoropoulou, K.T. McCarthy, S.B. Arnason, A.F. Hebard, S.N.G. Chu, R.G. Wilson, J.M. Zavada, Y.D. Park, J. Vac. Sci. Technol. B 20 (2002) 969.
[21] T. Dietl, H. Ohno, F. Matsukura, J. Cubert, D. Ferrand, Science 287 (2000) 1019.
[22] T. Dietl, A. Haury, Y. Merle d'Aubigne, Phys. Rev. B 55 (1997) R3347.
[23] M.L. Reed, N.A. El-Masry, H. Stadelmaier, M.E. Ritums, N.J. Reed, C.A. Parker, J.C. Roberts, S.M. Bedair, Appl. Phys. Lett. 79 (2001) 3473.
[24] N. Theodoropoulou, A.F. Hebard, M.E. Overberg, C.R. Abernathy, S.J. Pearton, S.N.G. Chu, R.G. Wilson, Appl. Phys. Lett. 78 (2001) 3475.
[25] S. Sonoda, S. Shimizu, T. Sasaki, Y. Yamamoto, H. Hori, J. Cryst. Growth 237–239 (2002) 1358;
T. Sasaki, S. Sonoda, Y. Yamamoto, K. Suga, S. Shimizu, K. Kindo, H. Hori, J. Appl. Phys. 91 (2002) 7911.
[26] G.T. Thaler, M.E. Overberg, B. Gila, R. Frazier, C.R. Abernathy, S.J. Pearton, J.S. Lee, S.Y. Lee, Y.D. Park, Z.G. Khim, J. Kim, F. Ren, Appl. Phys. Lett. 80 (2002) 3964.
[27] Park, H.-J. Lee, Y.C. Cho, S,-Y. Jeong, C.R. Cho, S. Cho, Appl. Phys. Lett. 80 (2002) 4187.
[28] M. Hashimoto, Y.-K. Zhou, M. Kanamura, H. Asahi, Solid State Commun. 122 (2002) 37.
[29] M.E. Overberg, C.R. Abernathy, S.J. Pearton, N.A. Theodoropoulou, K.T. McCarthy, A.F. Hebard, Appl. Phys. Lett. 79 (2001) 1312.
[30] K.H. Kim, K.J. Lee, D.J. Kim, H.J. Kim, Y.E. Ihm, D. Djayaprawira, M. Takahashi, C.S. Kim, C.G. Kim, S.H. Yoo, Appl. Phys. Lett. 82 (2003) 1775.
[31] S. Dhar, O. Brandt, A. Trampert, L. Daweriz, K.J. Friendland, K.H. Ploog, J. Keller, B. Beschoten, G. Guntherodt, Appl. Phys. Lett. 82 (2003) 2077.
[32] M. Jain, L. Kronik, J.R. Chelikowsky, V.V. Godlevsky, Phys. Rev. B 64 (2001) 245205.
[33] L. Kronik, M. Jain, J.R. Chelikowsky, Phys. Rev. B 66 (2002) R041203.
[34] Y.L. Soo, G. Kioseouglou, S. Kim, S. Huang, Y.H. Kaa, S. Kubarawa, S. Owa, T. Kondo, H. Munekata, Appl. Phys. Lett. 79 (2001) 3926;
M. Sato, H. Tanida, K. Kato, T. Sasaki, Y. Yamamoto, S. Sonoda, S. Shimiyu, H. Hori, J. Jap. Appl. Phys. 41 (2002) 4513.
[35] E. Kulatov, Phys. Rev. B 66 (2002) 045203.
[36] G.A. Medvedkin, T. Ishibashi, T. Nishi, K. Hiyata, Jap. J. Appl. Phys. 39 (2000) L949.
[37] M. Hashimoto, Y.-K. Zhou, M. Kanamura, H. Asahi, Solid State Commun. 122 (2002) 37.
[38] T. Fukumura, Z. Jin, M. Kawasaki, T. Shono, T. Hasegawa, S. Koshikara, S. Koshihara, H. Koinuma, Appl. Phys. Lett. 78 (2001) 958.

[39] S.G. Yang, A.B. Pakhomov, S.T. Hung, C.Y. Wong, Appl. Phys. Lett. 81 (2002) 2418.
[40] N. Theodoropoulou, A.F. Hebard, M.E. Overberg, C.R. Abernathy, S.J. Pearton, S.N.G. Chu, R.G. Wilson, Phys. Rev. Lett. 89 (2002) 107203-1.
[41] M.E. Overberg, B.P. Gila, G.T. Thaler, C.R. Abernathy, S.J. Pearton, N. Theodoropoulou, K.T. McCarthy, S.B. Arnason, A.F. Hebard, S.N.G. Chu, R.G. Wilson, J.M. Zavada, Y.D. Park, J. Vac. Sci. Technol. B 20 (2002) 969.
[42] S. Cho., S. Choi, G.B. Cha, S.C. Hong, Y. Kim, Y.-J. Zhao, A.J. Freeman, J.B. Ketterson, B.J. Kim, Y.C. Kim, B.C. Choi, Phys. Rev. Lett. 88 (2002) 257203-1.
[43] G.A. Medvedkin, T. Ishibashi, T. Nishi, K. Hiyata, Jap. J. Appl. Phys. 39 (2000) L949.
[44] S. Choi, G.B. Cha, S.C. Hong, S. Cho, Y. Kim, J.B. Ketterson, S.-Y. Jeong, G.C. Yi, Solid-State Commun. 122 (2002) 165.
[45] M.E. Overberg, C.R. Abernathy, N.A. Theodoropoulou, A.F. Hebard, S.N.G. Chu, A. Osinsky, V. Zuflyigin, L.D. Zhu, A.Y. Polyakov, R.G. Wilson, J. Appl. Phys. 92 (2002) 2047.
[46] N. Theodorpoulou, A.F. Hebard, S.N.G. Chu, M.E. Overberg, C.R. Abernathy, S.J. Pearton, R.G. Wilson, J.M. Zavada, Y.D. Park, J. Vac. Sci. Technol. A 20 (2002) 579.